



CHORUS

This is the accepted manuscript made available via CHORUS. The article has been published as:

Comment on “Isochoric, isobaric, and ultrafast conductivities of aluminum, lithium, and carbon in the warm dense matter regime”

B. B. L. Witte, G. Röpke, P. Neumayer, M. French, P. Sperling, V. Recoules, S. H. Glenzer,
and R. Redmer

Phys. Rev. E **99**, 047201 — Published 24 April 2019

DOI: [10.1103/PhysRevE.99.047201](https://doi.org/10.1103/PhysRevE.99.047201)

Comment on "Isochoric, isobaric, and ultrafast conductivities of aluminum, lithium, and carbon in the warm dense matter regime"

B. B. L. Witte,^{1,2} G. Röpke,¹ P. Neumayer,³ M. French,¹
P. Sperling,^{2,4,5} V. Recoules,⁶ S. H. Glenzer,² and R. Redmer¹

¹*Institut für Physik, Universität Rostock, 18051 Rostock, Germany*

²*SLAC National Accelerator Laboratory, 2575 Sand Hill Road, MS 72 Menlo Park, CA 94025 USA*

³*Extreme Matter Institute, GSI Helmholtzzentrum für Schwerionenforschung, Planckstr. 1, 64291 Darmstadt, Germany*

⁴*European XFEL, Holzkoppel 4, 22869 Schenefeld, Germany*

⁵*Aible GmbH, Am Vögenteich 24, 18055 Rostock, Germany*

⁶*CEA, DAM, DIF, 91297 Arpajon Cedex, France*

(Dated: March 27, 2019)

Dharma-wardana *et al.* [M. W. C. Dharma-wardana *et al.*, Phys. Rev. E **96**, 053206 (2017)] recently calculated dynamic electrical conductivities for warm dense matter as well as for nonequilibrium two-temperature states termed "ultrafast matter" (UFM) [M. W. C. Dharma-wardana, Phys. Rev. E **93**, 063205 (2016)]. In this comment we present two evident reasons, why these UFM calculations are neither suited to calculate dynamic conductivities nor x-ray Thomson scattering spectra in isochorically heated warm dense aluminum. First, the ion-ion structure factor, a major input into the conductivity and scattering spectra calculations, deviates strongly from that of isochorically heated aluminum. Second, the dynamic conductivity does not show a non-Drude behavior which is an essential prerequisite for a correct description of the absorption behavior in aluminum. Additionally, we clarify misinterpretations by Dharma-wardana *et al.* concerning the conductivity measurements of Gathers [G. R. Gathers, Int. J. Thermophys. **4**, 209 (1983)].

Recently, Dharma-wardana [1] and Dharma-wardana *et al.* [2] (both referred to as DWD in what follows) argued that the neutral pseudoatom (NPA) model can be applied to study matter isochorically heated by intense x-ray radiation to two-temperature states in strong non-equilibrium (ultra-fast matter: UFM). As a consequence a very low conductivity has been predicted to interpret the experiment [3]. Simultaneously, severe criticism was raised against two of our own studies on x-ray Thomson scattering (XRTS) spectra measured with the Linac Coherent Light Source (LCLS) [3] and their interpretation using state-of-the-art DFT-MD simulations [4]. Furthermore, our interpretation of electrical conductivity data σ from isobaric heating experiments of Gathers [5] has been questioned.

In this comment we address the criticism of DWD point by point [labeled **(i)** to **(viii)**] and show that the NPA model of DWD is not suited to describe the warm dense matter (WDM) regime, none of the points raised against our DFT-MD results are valid, and that our interpretation of the Gathers data [5], which are used to benchmark DFT-MD and NPA results, is correct.

Different approaches are known to calculate the dc conductivity σ in the WDM region. A general version of the Ziman formula used by DWD reads (Ref. [1], Eq. (3), and Ref. [6], Eqs. (2.1) and (2.9))

$$\frac{1}{\sigma} = \frac{\hbar}{3\pi Z e^2 n_e} \int_0^\infty d\varepsilon [-f'(\varepsilon)] \int_0^{2k} dq q^3 S_{ii}(q) \Sigma(q, k), \quad (1)$$

where $f'(\varepsilon)$ denotes the derivative of the Fermi function with respect to $\varepsilon = \hbar^2 k^2 / (2m)$, n_e the electron density, Z the average ion charge, $S_{ii}(q)$ the ion-ion structure factor, and $\Sigma(q, k)$ the scattering cross section of electrons by the

ions. In Born approximation where the scattering cross section is replaced by $|U_{ei}(q)/\epsilon(q)|^2$, the familiar form of the Ziman formula (Ref. [2], Eq. (A14)) is obtained.

(i) For an appropriate pseudopotential formfactor (Ashcroft pseudopotential) and a "spherically averaged $S(q)$ taken as a frozen fluid, say, at 0.06 eV" [1], the Ziman approach results in a conductivity of about 1×10^6 S/m [1, 2]. Both the weak-scattering approximation calculation (using the NPA pseudopotential) and a strong-scattering calculation (from the NPA phase shifts) for σ shown in Fig. 3 of Ref. [1] are significantly below the conductivity values of aluminum in the liquid state and, even more, in the solid state. DWD [1] argued that "this supports the picture where the WDM aluminum in the experiment is better modeled as a $2T$ UFM system". Note, that the expt. spectra [3] do not necessarily lead to this low conductivity value of about 1×10^6 S/m [7].

$S_{ii}(k)$ of isochorically heated aluminum has been determined in two experiments at the LCLS. Sperling *et al.* have measured XRTS spectra [3] in the seeded beam mode using a 10 μm focal spot size. With a normalization to the free electron density ($Z_f = 3$) of the inelastic scattering contribution the ion feature was determined, see Fig. 3 in [4]. Neumayer *et al.* have measured XRTS spectra [8] with a LCLS focal spot width of 50 μm in the SASE beam mode. Measurements were taken for scattering angles from 5° to 80° ($k = 0.35 \text{ \AA}^{-1}$ to $k = 5.2 \text{ \AA}^{-1}$) and at 150° ($k = 7.8 \text{ \AA}^{-1}$) in back scattering geometry. The calibration of the CCD camera was done by the free electron density in the inelastic scattering signal.

Qualitative agreement between the measured $S_{ii}(k)$ [3, 8] and the DFT-MD simulations is demonstrated in Fig. 1. The intensity of the diffuse background between the Laue diffraction peaks is sensitive to the ion temper-

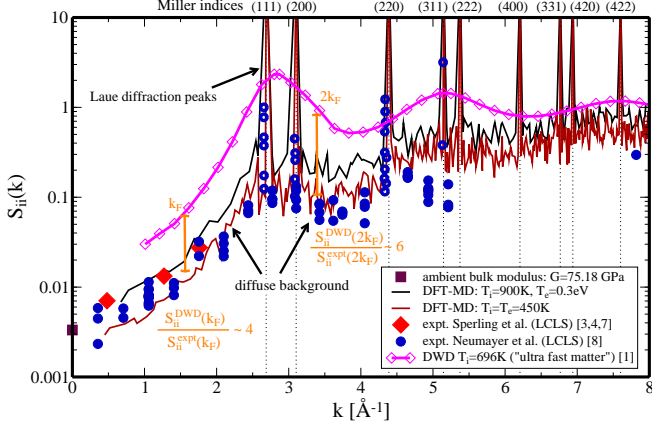


FIG. 1. $S_{ii}(k)$ of aluminum measured at LCLS by Sperling *et al.* [3] (red squares) and Neumayer *et al.* [8] (blue circles) within ultra-short 25-50 fs pulses in comparison with predictions of DWD [1] and DFT-MD.

ature [4]. The long wavelength limit of $S_{ii}(k)$ in isochorically heated aluminum is consistent with the bulk modulus 75.18 GPa of solid aluminum (magenta box) [9]. The lattice-like signatures (blue open circles [8]), consistent with the data from Fig. 4 of Ref. [10] cannot be described by the assumption of a liquid-like structure, see Fig. 1(b) in [1]. As the $S_{ii}(k)$ used by DWD differs strongly from the experiments, the quality of the conductivity according to Eq. (1) is questionable.

(ii) Furthermore, DWD [2] claim, "The excellent accord between our XRTS calculation and that of Witte *et al.* establishes that our $S(k)$, electron charge distributions, and potentials $U_{ei}(k)$ and $V_{ii}(k)$ are fully consistent with the structure data and electronic properties coming from DFT-MD simulations." This statement is invalid as shown above. In addition to the missing diffraction peaks, the UFM calculations overestimate the ion feature in forward direction. For instance, $S_{ii}(k)$ from DWD at $k = 1.5 \text{ \AA}^{-1}$ is more than a factor of two larger than the expt. data and the DFT-MD calculations, see Fig. 1. Another example can be taken from Fig. 3 of [4]. The ion feature at $k = 1.27 \text{ \AA}^{-1}$ was measured to be $|N(k)|^2 S(k) = 1.36$ which is equivalent to $S_{ii}(k = 1.27 \text{ \AA}^{-1}) = 0.01$ using $N(k = 1.27 \text{ \AA}^{-1}) = 11.5$ from e.g. [11–13] or DFT-MD. Thus, the elastic scattering as obtained by DWD in UFM at $k = 1.27 \text{ \AA}^{-1}$ is off by more than a factor of three compared to the experiments. We conclude that the UFM conductivity as calculated in [1, 2] are not reliable in this regime because the ion-ion structure factor is in disagreement with the expt. data [3, 8].

For the Ziman formula which can be derived from the autocorrelation function of stochastic forces, see [14], questions regarding Z or the electron-electron interactions [15] arise. With respect to the electron-ion interaction, the factorization in the formfactor and the ionic

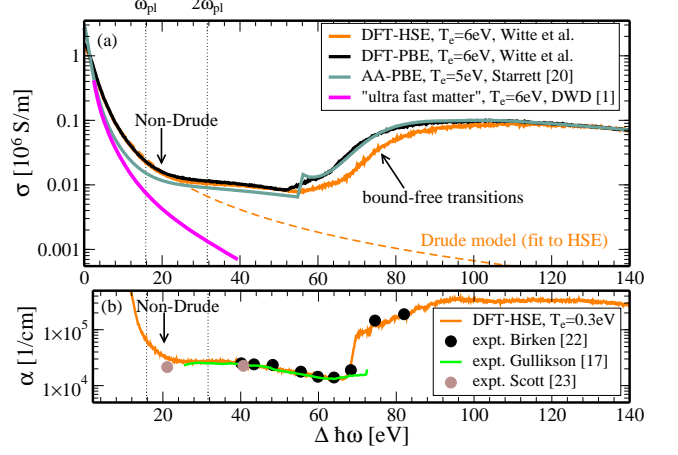


FIG. 2. (a): real part of σ in warm dense aluminum at $\rho=2.7 \text{ g/cm}^3$. The UFM-NPA model [1] does not capture non-Drude behavior in contrast to DFT-MD [4] or AA [20, 21]. (b): absorption coefficient shows non-Drude behavior in the dielectric function (compare Birken *et al.* [22], Gullikson *et al.* [17], Scott *et al.* [23]) appearing slightly above the plasma frequency, $\omega_{pl} = 15.8 \text{ eV}$ (Fig. taken from [7]).

structure factor (1) is exact only in Born approximation. For stronger interactions, DWD used the approximation of strong but isolated scatterers where the electron-ion formfactor is replaced by the differential scattering cross section, see Eq. (1). This factorization is not strictly valid, and one has to take into account the scattering of electrons by the whole ion subsystem as expressed by the corresponding multiple-scattering T matrix. It is obvious from Fig. 1, that Eq. (1) for the Ziman formula as used by DWD [1, 2] is not applicable for $S_{ii}(k)$ showing Laue diffraction peaks. Instead, the appropriate choice of single-particle states is inherent in the Kubo-Greenwood approach, which allows for the calculation of the conductivity without assuming ionization degrees, independent scattering centers, and avoiding perturbation approaches which are not justified in the limit of strong interactions. The conclusion of Ref. [1] that "the NPA phase-shift approach seems to be practically the only method currently available for including strong electron-ion collision effects in a reliable way" is certainly exaggerated.

(iii) To describe the XRTS spectra in isochorically heated aluminum DWD calculate the dynamic conductivity without considering its well-known non-Drude behavior which is reflected in the imaginary part of the dielectric function $\epsilon(\omega)$, in the real part of the absorption coefficient $\alpha(\omega)$, or in the real part of the dynamic conductivity $\sigma(\omega)$. Clear expt. evidence for this behavior is available [16, 17] which manifests in the appearance of a Cooper minimum [18, 19].

The plasmon shape of isochorically heated aluminum was measured at the LCLS [3, 4]. The maximum position

of the plasmon in the XRTS spectrum (see Fig. 4 in [1]) is located at frequency shifts of ~ 20 eV. In Fig. 2(a) we show that $\sigma(\omega)$ of the UFM model [1, 2] deviates at this frequency shift by a factor of about 5-10 from DFT or the average atom (AA) model [21]. This discrepancy is due to the lack of a non-Drude behavior in the UFM model. Thus, we have strong concerns that the interpretation of XRTS spectra for isochorically heated aluminum as done by DWD [1, 2] is correct. In Fig. 2(b) the expt. evidence for a non-Drude behavior is shown from the absorption coefficient (taken from [7]). We recognize, that DWD calculates the conductivity in a system with "cold" ions (2T), but we do not find any discussion why the non-Drude character should disappear in an even more structured system. Obviously, the NPA method is not capable of calculating this feature, even in equilibrium.

(iv) Notice that DWD misread the conductivity published by Sperling *et al.* [3], compare the real part of $\sigma(\omega)$ in Fig. 5 of [1] to the original data in [3] (inset of Fig. 3(b)). In Fig. 5 of [1] the conductivity ratio for frequencies at $0.5 \omega_{pl}$ and $2 \omega_{pl}$ is obviously $\frac{\sigma(0.5\omega_{pl})}{\sigma(2.0\omega_{pl})} > 10^3$ while the original data in [3] clearly yield $\frac{\sigma(0.5\omega_{pl})}{\sigma(2.0\omega_{pl})} < 10^2$. Consequently, the corresponding discussion of $\sigma(\omega)$ by DWD is flawed.

(v) In Fig. 3(a) we show that the NPA [2] differs strongly from the DFT-MD simulations [7] and the AA models [24, 25]: it does not reproduce the non-Drude behavior for $\sigma(\omega)$ in aluminum caused by the shape of the orbitals within the partially free states around the Fermi energy, while AA models and DFT capture this important feature [7]; thus we also reject the criticism on AA in subsection 3 of the appendix of Ref. [2]. Additionally, the strong deviations from other calculations and an experiment [26] for temperatures of $T \geq 10$ eV, where a local maximum instead of a minimum at about 25 eV occurs, might be caused by an overestimated ionization degree with increased temperature entering the NPA. Therefore, we consider the dc conductivities of the NPA method as questionable.

(vi) It is important to point out a misinterpretation of the conductivities measured by Gathers [5] for liquid aluminum in Ref. [2], where it reads: "*Gathers' tabulation and the several resistivities given are indeed a bit confusing*". In Fig. 3(b) we plot the data of column 4 and column 5 of table II from Gathers [5]. DWD interprets column 4 as the expt. measurement of isobarically heated aluminum. We give two reasons why only column 5 represents the isobaric measurement and why the numbers given in column 4 are rather crude estimates towards the isochoric liquid aluminum conductivity.

First, we compare with the review paper of Desai *et al.* [28] who reviewed 191 conductivity data sets available at that time (1984). In the liquid metal regime, they report only the isobaric conductivity as shown in Fig. 3(b). This data is consistent with column 5 of table II in Gathers [5] and deviates from NPA [2].

Second, it is straightforward to understand the scaling

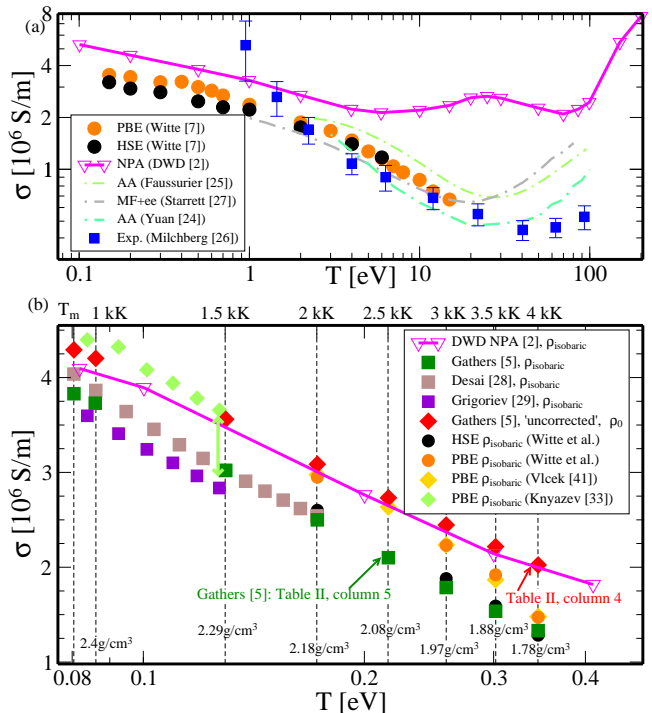


FIG. 3. (a): dc conductivity from DFT-MD simulations [7], the AA model [24, 25] and a mean field calculation [27] compared to the NPA of DWD [2] and expt. results of Milchberg *et al.* [26]. (b): Comparison of dc conductivities in isobaric aluminum from the NPA model [2] to expt. data. DWD claim good agreement with the Gathers points (red), although NPA predicts more than 20% higher conductivities compared to the isobaric measurements of Gathers [5] (green), Desai *et al.* [28] (brown) or Grigoriev *et al.* [29] (purple), cf. text.

of columns 4 and 5 by investigating the ratio between the two data sets. For instance, at $T = 1500$ K, column 5 reads $R = 0.331 \times 10^{-6} \Omega m$ and thus, $\sigma = 1/R = 3.02 \times 10^6$ S/m. Notice, that the mass density of isobaric aluminum at $T = 1500$ K is $\rho_{ib} = 2.29$ g/cm³; DWD and Witte *et al.* agree on this. Column 4 reads $R = 0.281 \times 10^{-6} \Omega m$ and, thus, $\sigma = 1/R = 3.56 \times 10^6$ S/m. The isochoric conductivity values ($\rho_{ic} = 2.70$ g/cm³) *uncorrected* from isobaric values as done by Gathers [5] can now be understood by a scaling according to the density: $\sigma_{ic} \approx \frac{\rho_{ic}}{\rho_{ib}} \sigma_{ib}$ and we get for this example $\sigma_{ic} \approx \frac{2.70}{2.29} \times 3.02 \times 10^6$ S/m = 3.56×10^6 S/m. This is fully consistent with column 4 of Gathers which represents the *uncorrected* values of the measured data to the isochoric (initial) density. It can easily be checked that the applied expansion scaling was done for all temperatures in table II, i.e., the green and red data in Fig. 3(b). We agree that this extrapolation to σ_{ic} made by Gathers might be crude and it takes careful reading to follow the description in [5, 30]. However, the isobaric measurements are given both by Desai *et al.* [28] and column 5 in table II of Gathers [5]; consistent with the data in [31] which are not in excellent agreement with the NPA. A

statement of Pottlacher *et al.* [32] on how to understand the meaning of the density uncorrected values is helpful in this context: "*The thermal uncorrected electrical resistivity is the resistivity calculated for a wire volume at room temperature and not for the actual volume.*" We strictly followed this direction when comparing with the data of Gathers [5] in our paper [4].

Furthermore, also Knyazev *et al.* [33] found that calculations with the PBE XC functional overestimate the dc conductivity in liquid aluminum by comparing to an isobaric data set [29], see Fig. 3(b). The deviation at $T \approx 1500$ K from PBE (comparable to NPA at that specific point) to the isobaric measurements is indicated with a green arrow. In [7] we have shown that the use of the HSE XC functional reduces the dc conductivity and results in better agreement with isobaric measurements compared to PBE or NPA.

(vii) Electronic conductivities from the DFT-MD method are calculated from the frequency-dependent Kubo-Greenwood formula [34–36]:

$$\lim_{k \rightarrow 0} \sigma(\omega) = \frac{2\pi e^2}{3\Omega\omega} \sum_{\mathbf{k}\nu\mu} (f_{\mathbf{k}\nu} - f_{\mathbf{k}\mu}) |\langle \mathbf{k}\nu | \hat{\mathbf{v}} | \mathbf{k}\mu \rangle|^2 \times \delta(E_{\mathbf{k}\mu} - E_{\mathbf{k}\nu} - \hbar\omega). \quad (2)$$

Extracting precise dc conductivities from Eq. (2) requires careful convergence tests with respect to, e.g., particle number N , \mathbf{k} -point grids, energy cutoff E_c , and a proper adjustment of the delta function broadening parameter [37] in order to perform the extrapolation to the dc value. Such tests were carefully made in all calculations presented in [4, 7, 38].

DWD finds larger dc conductivities from NPA-Ziman calculations compared to DFT and attributes this partly to the "*inability of the DFT-MD-KG approach to access small- k scattering contributions unless the number of atoms N in the simulation is sufficiently large.*" The criticism on Refs. [4, 38], however, is not valid. Note that several earlier studies reported well-converged conductivity calculations for aluminum and lithium with similar particle numbers [37, 39–41].

We show convergence tests in Fig. 4; in (a) $\sigma(\omega)$ as a function of E_c . Convergence is achieved with $E_c=500$ eV for the used GW-labeled 11-electron PAW potential. For $E_c=300$ eV $\sigma(\omega_{pl})$ is underestimated by 15%; see panel (b), where the relative difference to a calculation with $E_c=1000$ eV is plotted. In Ref. [2] an energy cutoff of 12 Ha (327 eV) was used in DFT. We also find that the dc limit of $\sigma(\omega)$ is up to 5% too high if E_c is too small. In panel (c) we display tests with respect to N and \mathbf{k} -point sampling. We obtain convergence for dc conductivities with $N=64$ at the Baldereschi-Mean-Value-Point (BMVP) when comparing to a calculation with $N=216$ and with $4 \times 4 \times 4$ Monkhorst-Pack (M444) \mathbf{k} -point sampling. In panel (d) we show our calculations of $S_{ii}(k)$ for $32 \leq N \leq 216$. The calculation using $N=32$ already results in a converged $S_{ii}(k)$, but smaller wavenumbers are accessible with $N=216$.

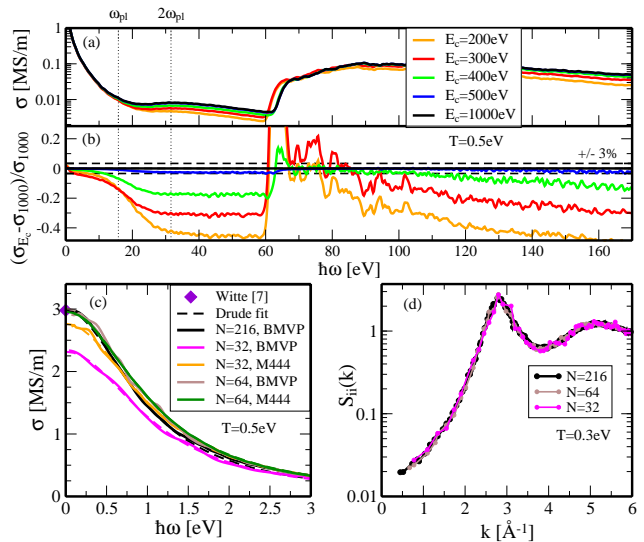


FIG. 4. Convergence test for DFT-MD simulations of liquid aluminum at solid density. (a): dynamic conductivity for different E_c and (b) relative deviation to the calculation with $E_c=1000$ eV. (c): dc conductivity convergence test for particle number and \mathbf{k} -point sampling. (d): convergence test of particle numbers for $S_{ii}(k)$.

We emphasize that it is generally not possible to transfer simulation parameters from one system to another. They depend strongly on the electronic and ionic structure, i.e. element, density, temperature, phase etc.; see [42–45]. The result of Pozzo *et al.* [43], who had to consider over 1000 atoms in order to get converged conductivities for liquid sodium, is an exception due to the proximity to the melt line ($T=400$ K) and by no means "*a case in point*" as DWD state. Several of the above references contain well-converged conductivities with 100 or less atoms.

(viii) DWD [2] criticize the choice of the exchange-correlation (XC) functional in Ref. [4]: "*Witte et al. strongly argue for the HSE functional even for aluminum, a simple metal proven to work well with more standard approaches, and propose that there are strong electron-electron interactions in Al.*" The HSE functional can remedy the band gap problem of the PBE functional and has proven useful for the calculation of electronic band gaps for semiconductors [46]. Although aluminum is a metallic system with no fundamental band gap, the imagination of it being a simple metal has limitations. As shown in Ref. [4, 7] and in this comment (Fig. 2(a)), $\sigma(\omega)$ shows a non-Drude behavior above ω_{pl} . This indicates that correlations between the conduction electrons are not negligible, cf. [7]. The simple approach of NPA [1, 2] is neither capable to reproduce a solid-like $S_{ii}(k)$ (see Fig. 1) nor a non-Drude conductivity as proven in [16, 17] of aluminum under ambient conditions. It therefore lacks the basis to give a reasonable description of aluminum in the regime of isochoric heating.

We conclude that some of the results given in Refs. [1,

2] are questionable. The calculation of XRTS spectra and conductivities for UFM are based on an unrealistic $S_{ii}(k)$ which does not correctly describe isochorically heated aluminum as prepared at the LCLS experiments. A non-Drude behavior in the $\sigma(\omega)$ of aluminum is not considered which indicates a lack of important physics in the NPA model or unsuited input parameters. Further, it was shown in Ref. [7] and in Fig. 3 that the difference in conductivity of liquid aluminum between the PBE and HSE functionals is significant. The better agreement of the HSE conductivities with the expt. results supports the usefulness of the HSE functional also in Kubo-Greenwood calculations for metallic systems. Other misconceptions

and errors in Ref. [2] and in Ref. [1] are clarified as well.

Acknowledgements. The authors thank C. Starrett for providing non-Drude conductivities from AA calculations for warm dense aluminum. We thank C. Dharma-wardana for the continuing interest in our work and for stimulating discussions. However, we were not able to resolve some issues which are addressed in this comment. The *ab initio* calculations were performed at the North-German Supercomputing Alliance (HLRN) facilities. This work was supported by the DFG within the SFB 652 and the FOR 2440, and by the DOE Office of Science, Fusion Energy Science under FWP 100182.

-
- [1] M. W. C. Dharma-wardana, Phys. Rev. E **93**, 063205 (2016).
- [2] M. W. C. Dharma-wardana, D. D. Klug, L. Harbour, and L. J. Lewis, Phys. Rev. E **96**, 053206 (2017).
- [3] P. Sperling, E. J. Gamboa, H. K. Chung, E. Galtier, H. J. Lee, Y. Omarbakiyeva, H. Reinholz, G. Röpke, U. Zastra, J. Hastings, L. B. Fletcher, and S. H. Glenzer, Phys. Rev. Lett. **115**, 115001 (2015).
- [4] B. B. L. Witte, L. B. Fletcher, E. Galtier, E. Gamboa, H. J. Lee, U. Zastra, R. Redmer, S. H. Glenzer, and P. Sperling, Phys. Rev. Lett. **118**, 225001 (2017).
- [5] G. R. Gathers, Int. J. Thermophys. **4**, 209 (1983).
- [6] F. Perrot and M. W. C. Dharma-wardana, Phys. Rev. A **36**, 238 (1987).
- [7] B. B. L. Witte, P. Sperling, M. French, V. Recoules, S. H. Glenzer, and R. Redmer, Physics of Plasmas **25**, 056901 (2018).
- [8] P. Neumayer, private communication, data from experiment L592 at LCLS (2016).
- [9] F. Cardarelli, "Materials Handbook: A Concise Desktop Reference," Springer, London, New York (2000).
- [10] L. B. Fletcher, H. J. Lee, T. Döppner, E. Galtier, B. Nagler, P. Heimann, C. Fortmann, S. LePape, T. Ma, M. Millot, A. Pak, D. Turnbull, D. A. Chapman, D. O. Gericke, J. Vorberger, T. White, G. Gregori, M. Wei, B. Barbrel, R. W. Falcone, C.-C. Kao, H. Nuhn, J. Welch, U. Zastra, P. Neumayer, J. B. Hastings, and S. H. Glenzer, Nat. Photonics **9**, 274 (2015).
- [11] L. Pauling and J. Sherman, Zeitschrift für Kristallographie **81**, 1 (1932).
- [12] J. H. Hubbell, W. J. Veigele, E. A. Briggs, R. T. Brown, D. T. Cromer, and R. J. Howerton, Journal of Physical and Chemical Reference Data **4**, 471 (1975).
- [13] D. A. Chapman, J. Vorberger, L. B. Fletcher, R. A. Baggott, L. Divol, T. Döppner, R. W. Falcone, S. H. Glenzer, G. Gregori, T. M. Guymer, A. L. Kritcher, O. L. Landen, T. Ma, A. E. Pak, and D. O. Gericke, Nature Communications **6**, 6839 EP (2015).
- [14] G. Röpke, Theoretical and Mathematical Physics **194**, 74 (2018).
- [15] M. P. Desjarlais, C. R. Scullard, L. X. Benedict, H. D. Whitley, and R. Redmer, Phys. Rev. E **95**, 033203 (2017).
- [16] B. L. Henke, E. M. Gullikson, and J. C. Davis, Atomic data and nuclear data tables **54**, 181 (1993).
- [17] E. M. Gullikson, P. Denham, S. Mrowka, and J. H. Underwood, Phys. Rev. B **49**, 16283 (1994).
- [18] U. Fano and J. W. Cooper, Rev. Mod. Phys. **40**, 441 (1968).
- [19] S. T. Manson, Phys. Rev. A **31**, 3698 (1985).
- [20] C. Starrett, private communication (2017).
- [21] C. E. Starrett, J. Clerouin, V. Recoules, J. D. Kress, L. A. Collins, and D. E. Hanson, Phys. Plasmas **19**, 102709 (2012).
- [22] H.-G. Birken, W. Jark, C. Kunz, and R. Wolf, Instrum. Methods Res. Sect. A **253** (1986).
- [23] M. L. Scott, P. N. Arendt, B. J. Cameron, J. M. Saber, and B. E. Newnam, Appl. Opt. **27**, 1503 (1988).
- [24] J. K. Yuan, Y. S. Sun, and S. T. Zheng, Phys. Rev. E **53**, 1059 (1996).
- [25] G. Faussurier and C. Blancard, Phys. Rev. E **91**, 013105 (2015).
- [26] H. M. Milchberg, R. R. Freeman, S. C. Davey, and R. M. More, Phys. Rev. Lett. **61**, 2364 (1988).
- [27] C. Starrett, High Energy Density Physics **25**, 8 (2017).
- [28] P. D. Desai, H. M. James, and C. Y. Ho, J. Phys. Chem. Ref. Data **13**, 1131 (1984).
- [29] I. Grigoriev and E. Meylikhov, (Eds.), Physical Quantities, Energoatomizdat, Moscow (1991).
- [30] G. R. Gathers, Rep. Prog. Phys. **49**, 341 (1986).
- [31] M. Leitner, T. Leitner, A. Schmon, K. Aziz, and G. Pottlacher, Metallurgical and Materials Transactions A **48**, 3036 (2017).
- [32] G. Pottlacher, T. Neger, and H. Jäger, High Temperatures - High Pressures **23**, 43 (1991).
- [33] D. Knyazev and P. Levashov, Computational Materials Science **79**, 817 (2013).
- [34] R. Kubo, J. Phys. Soc. Jpn. **12**, 570 (1957).
- [35] D. A. Greenwood, Proc. Phys. Soc. **71**, 585 (1958).
- [36] B. Holst, M. French, and R. Redmer, Phys. Rev. B **83**, 235120 (2011).
- [37] M. P. Desjarlais, J. D. Kress, and L. A. Collins, Phys. Rev. E **66**, 025401 (2002).
- [38] B. B. L. Witte, M. Shihab, S. H. Glenzer, and R. Redmer, Phys. Rev. B **95**, 144105 (2017).
- [39] V. Recoules and J. P. Crocombette, Phys. Rev. B **72**, 104202 (2005).
- [40] A. Kietzmann, R. Redmer, M. P. Desjarlais, and T. R. Mattsson, Phys. Rev. Lett. **101**, 070401 (2008).
- [41] V. Vlček, N. de Koker, and G. Steinle-Neumann, Phys.

- Rev. B **85**, 184201 (2012).
- [42] M. French, T. R. Mattsson, and R. Redmer, Phys. Rev. B **82**, 174108 (2010).
- [43] M. Pozzo, M. Desjarlais, and D. Alfè, Phys. Rev. B **84**, 054203 (2011).
- [44] D. Alfè, M. Pozzo, and M. P. Desjarlais, Phys. Rev. B **85**, 024102 (2012).
- [45] M. French and T. R. Mattsson, Phys. Rev. B **90**, 165113 (2014).
- [46] J. Heyd, J. E. Peralta, G. E. Scuseria, and R. L. Martin, J. Chem. Phys. **123**, 174101 (2005).